Optik 157 (2018) 1115–1121

Contents lists available at ScienceDirect

Optik

journal homepage: www.elsevier.de/ijleo

Original research article

Effect of annealing temperature on optical properties of silver-PVA nanocomposite

Sulochana Deb*, Deepali Sarkar

Department of Physics, Gauhati University, Guwahati, Assam, 781014, India

ARTICLE INFO

Article history:
Received 16 June 2017
Received in revised form 31 October 2017
Accepted 19 November 2017

Keywords:
Annealing
Silver nanoparticles
Plsmon resonance
Polymer composite

ABSTRACT

The present article reports the effect of annealing temperature on the morphology and optical properties of silver nanoparticles embedded in polyvinyl alcohol (PVA) matrix. The nanocomposite films prior to annealing shows spherical grains. These films are annealed at five different temperatures (373 K, 423 K, 473 K, 523 K and 573 K) in vacuum and the effects on surface morphology and optical properties are investigated. The unannealed and annealed films are characterized by FESEM, XRD, FTIR spectra, TGA, UV–vis absorption spectra and photoluminescence (PL) spectra. Scanning electron microscopy images show the change in shape and size with increase of annealing temperature. Spherical shapes of the grains in pre annealed samples get changed to nanocubes and nanorods at higher annealing temperatures of 523 K and 573 K respectively. UV–vis spectra show a remarkable change of surface plasmon resonance peak with the increase in annealing temperature. XRD shows a characteristic intense peak of silver nano at $2\theta = 38^0$ for (111) crystalline plane with no significant change with annealing temperature. Photoluminescence spectra show a tendency of red shift of emission peak.

1. Introduction

Plasmonic metal nanoparticles specially silver nano-sized particles have drawn much attention for their unique electrical, optical, antimicrobial and biological properties [1–7]. Silver nanoparticles give typical absorption spectra due to surface Plasmon resonance (SPR) arising from oscillation of conduction electrons which depend upon the size and shape of the particles [8]. Silver exhibit highest efficiency of plasmon excitation [9] and SPR can be tuned to any desired wavelength in the visible region which makes them suitable for a variety of applications including sensors, colour filters and waveguides [10,11]. Various methods have been reported for synthesis of silver nanoparticles such as embedding nanoparticles in glass [12], silica [13] or polymers [14–18]. Use of synthetic high polymer such as polyvinyl alcohol (PVA), polyacrylic acid or polymethyl methacrylate etc. are of particular great interest as the polymers prevent oxidation and coalescence of the particles and provide them long time stability [19,20]. PVA could be considered as a good host material for metal due to its excellent elasticity, transparency, thermo stability, chemical resistance, high mechanical strength, water solubility, and moderate and dopant dependent electrical conductivity which make them suitable for many industrial applications such as coating, enjyme immobolization, reinforcement etc. [21–26]. The optical and electrical properties of the nanoparticles can be brought into full play, while the typical advantages of organic polymers are retained in the composite films. As the

* Corresponding author.
E-mail address: debsulochana@gmail.com (S. Deb).

https://doi.org/10.1016/j.ijleo.2017.11.112
0030-4026/

physical, chemical and optical properties of the nanoparticles are often found to be dependent on their size and shape, so numerous methods are developed to manipulate the size and shape viz. changing the concentration of the starting materials in chemical reduction [27,28], using templates [29], changing matrix, changing temperature of synthesis, photoreduction method [30,31], post synthesis annealing [32–34] etc. Annealing is well known to bring more order in the system by changing the particle size, orientation, alignment etc. to give lesser entropy state. After annealing the morphology of the nanoparticles changes subsequently resulting in shift of SPR peak [33–35]. SPR intensity is dependent on density of nanoparticles [36]. On annealing there can be change in size and thence density of particles which will be reflected in SPR peak intensity. Annealing process also affects in the floating silver nanoparticles which are applied in Organic Non Volatile memory transistors [37]. In general one can say that various physical properties can be maneuvered by annealing process. Such nanocomposites can be used as promising materials for novel functional applications in plasmonics and photonics. In the present article, we report the effect of annealing on the surface morphology with formation of nanocubes and nanorods and optical properties of silver nanoparticles synthesized by chemical reduction method. Morphology of the particles are observed through FESEM measurements whereas optical properties through UV–vis and photoluminescence spectra. Heat treatment induced changes observed in UV–vis and photoluminescence have been correlated to the size and shape of silver nanoparticles.

2. Experimental

2.1. Materials used

Materials used for the present fabrication process are polyvinyl alchohol (PVA) and silver nitrate ($AgNO_3$). PVA (1700–1800 repeat units) is obtained from Sigma Chemical Co. and is of very high purity (99.9%). Silver nitrate of 99.9% purity is obtained from E. Merk, Germany. These materials are used without any further purification.

2.2. Method of synthesis and characterizations

Silver-PVA nanostructured films are prepared by chemical reduction of silver in presence of aqueous PVA as has been detailed in some earlier works [27]. To be particular, Silver nitrate (1 mM) solution is added to PVA solution (3 wt%) with constant stirring at 90 °C. The solution is maintained at that temperatute for1hr. for the formation of silver nano, indicated by the change in colour of the solution to light yellow. This solution is spin cast and dried in vacuum for further investigations.Obtained films show presence of spherical particles which are confirmed to be silver in homogeneous background of PVA. These composite films containing spherical silver nanoparticles are annealed at different temperatures ranging from 373 K to 573 K in vacuum. Formation mechanism of silver nanorods is shown in Fig. 1. The grain size increases with the increase in annealing temperature due to coalescence of the particles and also increase in annealing temperature leads to increase the crystallinity of the material. Similar result is obtained in [38–40]. Significant change in size and shape is observed at annealing temperature 523 K and 573 K. This can be correlated to the pyrolysis of the nanocomposite occurring at around 523 K as observed in TGA. Characterization of the annealed films is done by FESEM, XRD, FTIR spectra, UV–vis absorption spectra and photoluminescence (PL) spectra. Thermal properties of the hybrid are investigated though TGA. Morphology and particle size determination of the composite film is done by field emission scanning electron microscope (SEM) (JSM-6360(JEOL)).XRD data for structure study are collected by Scifert XRD 3000 pd Diffractometer with Cu-K_α (0.15418 nm) radiation. FTIR spectra are taken by Bruker Alpha ATR spectrometer. TGA analysis is done by Mettler Toledo,TGA/DSC-1, star System. UV–vis absorption and Photoluminescence (PL) studies are done by Carry-300 spectrophotometer and F-2500 FL Spectrometer respectively.

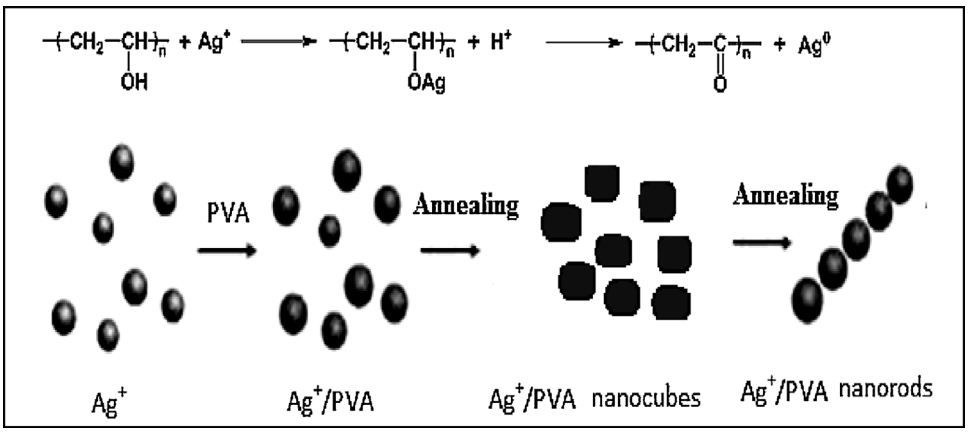

Fig. 1. Formation mechanism of nanorods.

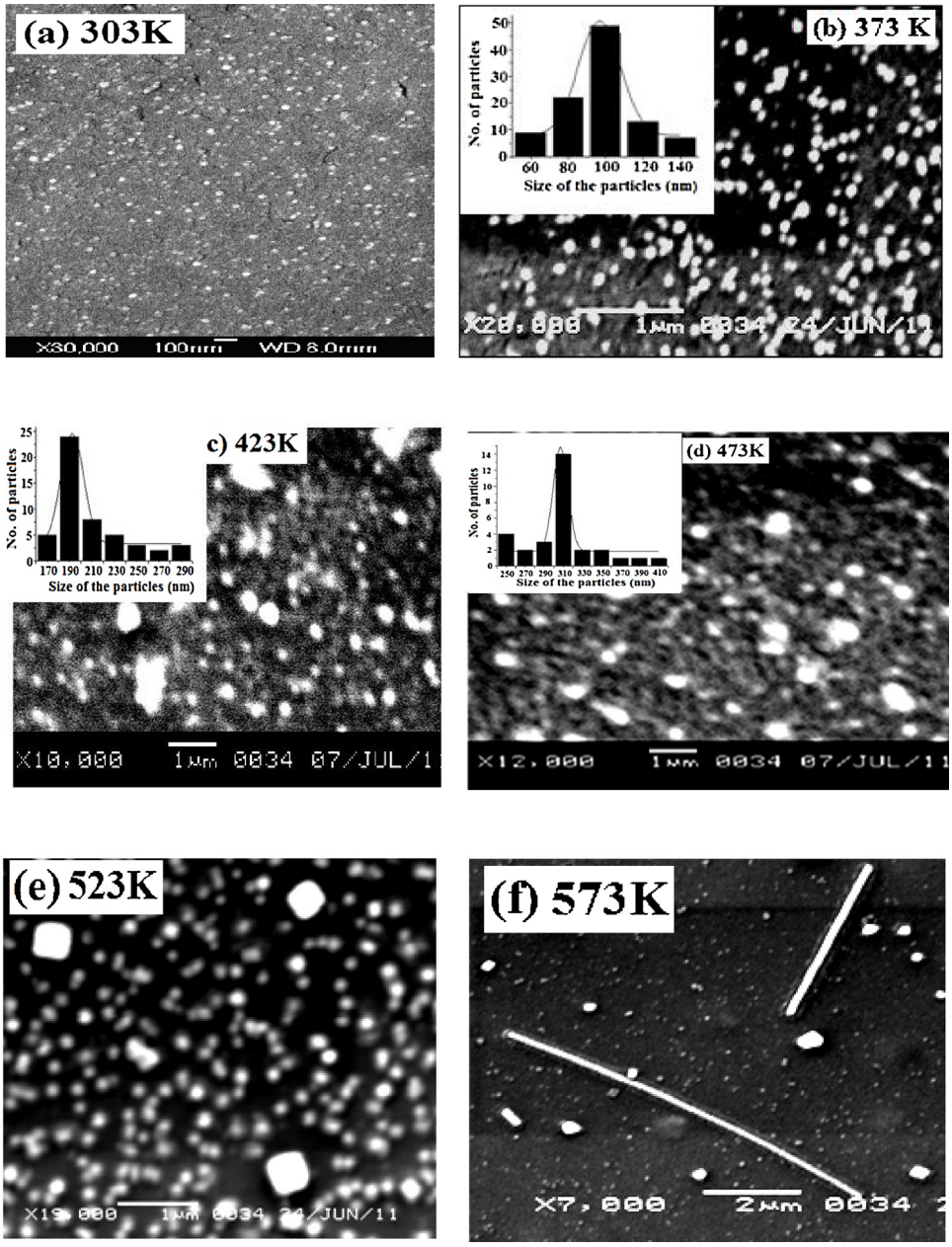

Fig. 2. SEM images of the samples: unannealed (a), and annealed at 373 K (b), 423 K (c), 473 K (d), 523 K (e), 573 K (f).

3. RESULTS & DISCUSSIONS

3.1. Morphology

The film morphology and particle size distribution of Ag-PVA nanocmposite films both annealed and unannealed are shown in Fig. 2(a–f). Average size of the particles obtained from histograms of these pictures is seen to increase from 100 nm–400 nm with the increase in annealing temperature. Also, in two of the cases of higher annealing temperatures, i.e. for 523 and 573 K, we observed formation of nanocubes and nanorods respectively as observed. This is quite justified as the morphological evolution in terms of change in size and shape and ordering of grains is known to be facilitated by annealing [33]. The average size of the nanocubes obtained at annealing temperature of 523 K is in the range of 200–400 nm. The length of the nanorods obtained for 573 K is in micrometer range whereas the average diameter is in the nanometer range. It is to be mentioned that the unannealed films show predominance of near-spherical particles of average particle diameter of 20 nm [41].

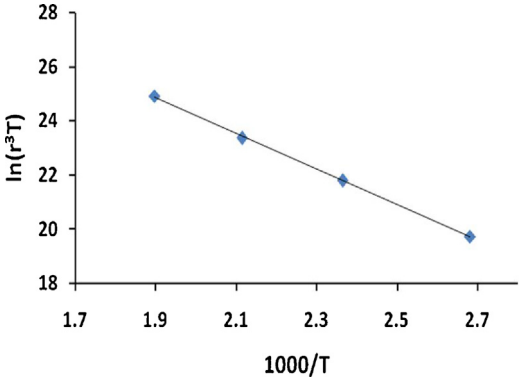

Fig. 3. Linear fit plot of ln(r^3T) vs. 1000/T.

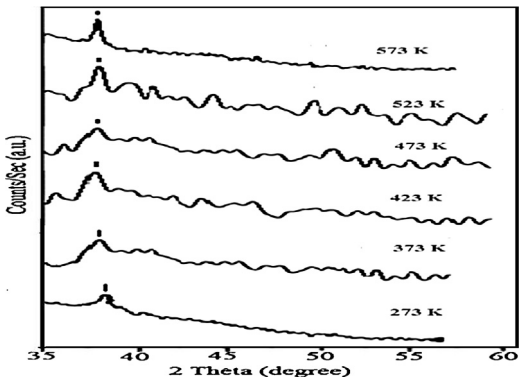

Fig. 4. XRD spectra of the samples unannealed and annealed at 373 K, 423 K, 473 K, 523 K, 573 K.

The average particle size obtained from the SEM image can related to annealing temperature for constant heat treatment time by the following equations [32]:

$$r = \exp(1/3(-\Delta E/RT - \ln T + \text{constant}))$$

where, r is the particle size, ΔE is the activation energy and R is ideal gas constant. In Fig. 3, we show a graph between ln (r^3T) vs. 1000/T for annealing temperatures 373 K to 523 K.

3.2. Xrd

XRD pattern of the nanocomposite films are shown in Fig. 4. This shows characteristic peak of silver nano at $2\theta = 38.02^0$ for (111) crystalline plane [39] with no significant change except increase in crystallinity with annealing temperature. The broad nature of the XRD peak could be attributed to formation of nanosized particles.

3.3. FTIR spectra

To look for the change in possible chemical bonding between the PVA and silver in the nanocomposite, FTIR spectra of unannealed and annealed samples at five different annealing temperatures are taken. These FTIR spectra are shown in Fig. 5. The vibrational peak at 3298, 2933, 1421 and 844 cm^{-1} are assigned to O—H stretching, C—H stretching, C—H bend of CH_2 and out of plane vibration of C—H group [40,42] Further, the vibrational peaks found in the range 1130–650 cm^{-1} may be attributed to Ag—O, which indicate that silver nanoparticles doped in the PVA polymer matrix [43]. These peaks are slightly shifted and intensity of these peaks are changed with increase in annealing temperature. The changes are prominent at temperature 523 K and 573 K.

3.4. Thermo-gravy metric analysis (TGA)

Thermal decomposition of the unannealed (6.8 mg) and annealed (7.6 mg) nanocomposites are studied through TGA curves. Decomposition profiles were obtained while heating at a rate of 10 °C/min in air between 25 °C and 700 °C. The relation between temperature and weight loss of the samples in the TGA curve is shown in Fig. 6. The initial weight loss

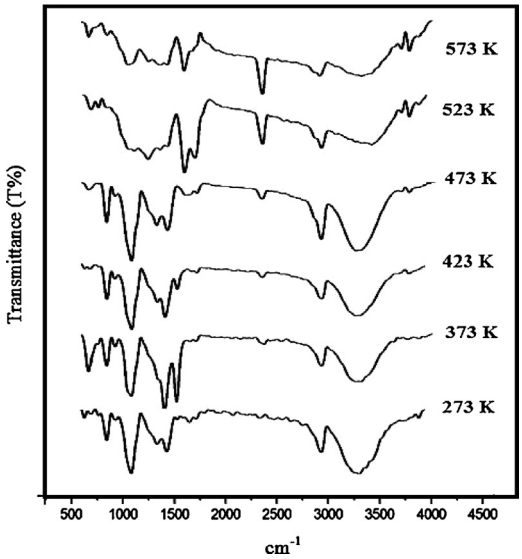

Fig. 5. FTIR spectra of the samples unannealed and annealed at 373 K, 423 K, 473 K, 523 K, 573 K.

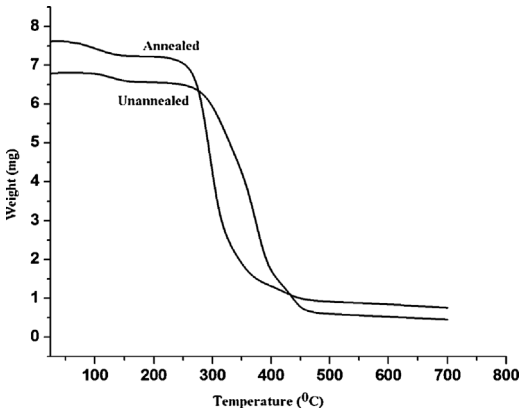

Fig. 6. Thermo-gravy metric analysis of the unannealed and annealed samples.

from 51 °C to 130 °C is attributed to the vaporization of the absorbed surface and interlayer water. The decrease of amount after the pyrolysis of the sample was 4.55% (0.3088 mg) for unannealed sample and 5.06% (0.3850 mg) for annealed sample. Thermogram shows that the PVA stabilized silver nanocomposite is thermally stable until 250 °C. Then, the material continues its degradation as the temperature is increased. The improvement of thermal stability of the PVA-stabilized silver nanocomposite is also reported by [44]. The end product after the pyrolysis is carbon coated silver nanoparticles [45] and the decrease in weight percentage is 88.8% (6.03 mg) for unannealed sample and 85% (6.4 mg) for annealed sample. The carbon coated silver nanoparticles do not evaporate at the temperature range between 498 °C and 700 °C. No change is observed with the increase in annealing temperature.

3.5. Optical properties

In Fig. 7, we show the UV–vis absorption spectra for these nanocomposite films for unannealed and annealed samples at five different annealing temperatures. These show strong plasmon resonance peak which is a clear consequence of formation of nano sized particles [46]. The size and shape of the particles are supposed to have a great impact on the UV–vis absorption spectra. The unannealed film shows peak at 441 nm as has been reported in our earlier work [41]. With the increase in annealing temperature, the surface Plasmon peak position is seen to get blue shifted. It can be observed that for the samples annealed at 373 K, the peak position is shifted to 410 nm. For samples annealed at 523 K, multiple peaks are observed. This is due to the fact that for the particle size greater than few hundred nanometer, the field across the particle becomes non-uniform and there is phase retardation which broadens the dipole resonance and excited higher multiple resonance, such as the qudrapole, octapole etc. leading to several peaks in the spectra [47,48]. For samples annealed at 573 K, The peak at 320 nm belongs to the optical signatures of silver nanorods [49]. Presence of small hump at around 440 nm in this sample is

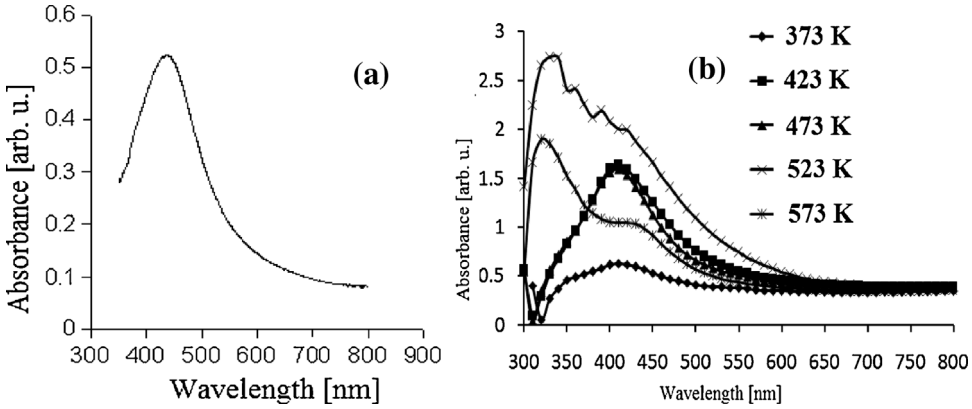

Fig. 7. Surface Plasmon Resonance spectra of the samples (a) before annealing and (b) after annealing at different temperatures.

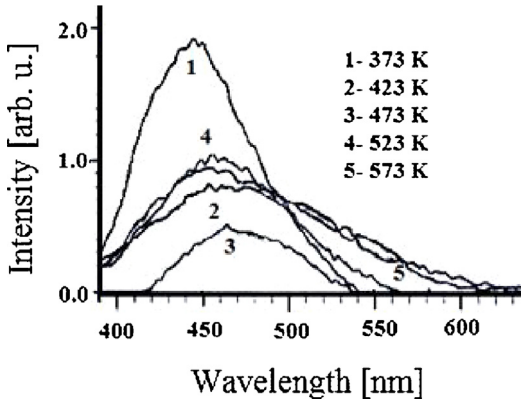

Fig. 8. Photoluminescence spectra of the samples after annealing at different temperatures.

due to the presence of spherical shaped nanoparticles along with the rods. The position of Plasmon absorption band depends on particle size, aspect ratio and diameter of nanowires or nanorods [44]. In this case, the broad absorption band exhibits that the final product should be the presence of both silver nanorods and dispersive particles [49]. This behavior may be justified as there is change in shape to cubic and rod at these temperatures as evident from the FESEM pictures discussed earlier.

In Fig. 8, we show the room temperature photoluminescence (PL) spectra of these annealed composite films for excitation wavelength of 350 nm. These show emission band at 445–465 nm Also there is an increase in fullwidth at half maxima (FWHM) value from 72 nm to 140 nm with increase of annealing temperature from 373 K to 573 K. Photoluminescence (PL) of silver is generally attributed to electronic transitions between the upper d band and conduction sp band [50]. For unannealed samples, there is no PL emission for this particular excitation wavelength but shows PL for excitation wavelength of 405–475 nm as reported in our earlier work [41]. PL intensity, peak position and broadening depends on the size of the nanoparticles [51]. These results suggest annealing induced colour tunable emission. In order to corroborate whether the PL emission is from the embedded Ag nanoparticles or from the parent compound (PVA), PL spectra for pure PVA film is measured and this shows no emission band. The absence of emission band at this region indicates PL emission to be originating from silver nanoparticles. Also, there is a trend of red shifting of PL peaks with annealing though these changes are not that in sequence with annealing temperature.

4. Conclusions

The Ag-PVA nanostructured nancomposite films on annealing show remarkable changes in morphological and optical properties. There is remarkable change in size and shape of nanoparticles on annealing. In the unannealed film, shape of the particles is mostly spherical. With the increase in annealing temperature the size is increase and also in one case formation of nanorod is observed by aligned assembly of nanoparticles. XRD spectra reveals increase crystallinity with the increase in annealing temperature. In FTIR specta, peaks correspond to molecular vibrations and chemical bonds, indicate the crosslinking of silver and PVA polymer. The shift in peak position and change in intensity of peak is observed with the increase in annealing temperature which is significant at 523 k and 573 K. Thermogravimetric studies have been performed to analyze the pyrolysis of the PVA-stabilized silver nanocomposite and it is observed that the decomposition of the compositeis

correlated formation mechanism and FTIR spectra. The A clear blue shift in surface plasmon resonance peak is observed with the increase of annealing temperature. The observed blue shift correlates well with the geometrical and dimensional changes of silver nanoparticles as revealed by SEM analysis. This study offers an interesting approach to alter surface Plasmon resonance characteristics and thus optical transmission properties of metal nanoparticles. Photoluminescence spectra also show trend of red shift and broadening with increase of annealing temperature.

Acknowledgements

The authors express their deep sense of gratitude to SAIF, NEHU, Shillong for SEM measurement, Dept. of Chemistry, Handique college, Guwahati for measurements of FTIR, Dept. of USIC,Gauhati University for measurements of XRD and Dept. of Chemistry, Gauhati University for measurements of PL spectra and TGA.

References

[1] N.N. Lepeshkin, A. Schweinsberg, G. Pivedda, R.S. Bennink, R.W. Boyd, Phys. Rev. Lett. 93 (2004) 123902, http://dx.doi.org/10.1103/PhysRevLett.93.123902.
[2] S. Horiuchi, T. Fujita, T. Hayakawa, Y. Nakao, Adv. Mater. 15 (2003) 1449–1452, http://dx.doi.org/10.1002/adma.200305270.
[3] B. Kang, J.W. Wu, J. Korean Phys. Soc. 49 (2006) 955–958, http://dx.doi.org/10.3938/jkps.49.955.
[4] K.H. Ng, H.R. Lin, M. Pennon, Langmuir 16 (2000) 4016–4023, http://dx.doi.org/10.1021/la9914716.
[5] S. Deb, D. Sarkar, J. Exp. Nanosci. 9 (2014) 375–381, http://dx.doi.org/10.1080/17458080.2012.661475.
[6] D. Saikia, P.K. Gogoi, P. Phukan, N. Bhuyan, S. Borchetia, J Adv. Mater. Lett. 6 (2015) 260–264, http://dx.doi.org/10.5185/amlett.2015.5655.
[7] B. Kumar, S. Kumari, A. Debut, J. Camacho, E.H. Gallegos, M. Chávez-López, M. Grijalva, Y. Angulo, G. Rosero, Adv. Mater. Lett. 6 (2015) 127–132, http://dx.doi.org/10.5185/amlett.2015.5697.
[8] I. Pastoriza- Santos, L. Liz- Marzan, Langmuir 18 (2002) 2888–2894, http://dx.doi.org/10.1021/la015578g.
[9] D.D. Evanoff, G. Chumanov, Chemphyschem 6 (2005) 1221, http://dx.doi.org/10.1002/cphc.200500113.
[10] A. Stalmashonak, G. Seifert, A. Abdolvand, Ultra-Short Pulsed Laser Engineered Metal-Glass Nanocomposites, Verlag: Springer, 2013, http://dx.doi.org/10.1007/978-3-319-00437-2.
[11] S. Mohapatra, J. Alloys Comp. 598 (2014) 11, http://dx.doi.org/10.1016/j.jallcom.2014.02.021.
[12] T. Tokijabi, A. Nakamura, S. Kaneko, K. Uchida, S. Omi, H. Tanji, Y. Asahara, Appl. Phy. Lett. 65 (1994) 941–943, http://dx.doi.org/10.1063/1.112155.
[13] I. Tanahashi, T. Mitsuyu, J. Noncryst. Solids 181 (1995) 77–82, http://dx.doi.org/10.1016/0022-3093(94)00498-6.
[14] Z.M. Mbhele, M.G. Sakmane, C.G.C.E. Van Sittert, J.M. Nedeljkovic, V. Djokovic, A.S. Luyt, Chem. Mater. 15 (2003) 5019–5024, http://dx.doi.org/10.1021/cm034505a.
[15] R. Zeng, M.G. Rong, M.Q. Zhang, H.C. Liang, H.M. Zeng, Appl. Surf. Sci. 187 (2002) 239–247, http://dx.doi.org/10.1016/S0169-4332(01)00991-6.
[16] Z. Zhang, M. Han, J. Mater. Commun. 13 (2003) 641–643, http://dx.doi.org/10.1039/B212428A.
[17] H. Liu, X. Ge, Y. Zhu, X. Xu, Z. Zhang, M. Zhan, Mater. Lett. 46 (2000) 205–208, http://dx.doi.org/10.1016/S0167-577X(00)00170-1.
[18] A.V. Firth, S.W. Haggata, P.K. Khanna, S.J. Williams, J.W. Allen, S.W. Magennis, I.D.W. Samuel, D.J. cole-Hamilton, J. Lumin. 109 (2004) 163–172, http://dx.doi.org/10.1016/j.jlumin.2004.02.004.
[19] A.N. Ananth, S. Umapathy, Appl. Nanosci. 1 (2) (2011) 87–96, http://dx.doi.org/10.1007/s13204-011-0010-7.
[20] P.K. Khanna, R. Gokhale, V.V.V.S. Subbarao, A.K. Vishwanath, B.K. Das, C.V.V. Satyanarayana, Mater. Chem. Phys. 92 (1) (2005) 229–233, http://dx.doi.org/10.1016/j.matchemphys.2005.01.016.
[21] G. Fussell, J. Thomas, J. Scanlon, A. Lowman, M. Marcolongo, J. Biomater. Sci. 16 (4) (2005) 489–503, http://dx.doi.org/10.1163/1568562053700219.
[22] S. Mallakpour, M. Dinari, J. Macromol. Sci. Part B 52 (11) (2016) 1651–1661, http://dx.doi.org/10.1080/00222348.2013.789349.
[23] S. Mallakpour, M. Dinari, Prog. Org. Coat. 77 (2014) 583–589, http://dx.doi.org/10.1016/j.porgcoat.2013.11.021.
[24] X. Sun, Y. Xin, X. Wang, H. Uyama, Colloid. Polym. Sci. 295 (2017) 1827–1833, http://dx.doi.org/10.1007/s00396-017-4160-3.
[25] S. Mallakpour, M. Dinari, J. Appl. Polym. Sci. 124 (2012) 4322–4330, http://dx.doi.org/10.1002/app.35540.
[26] S. Mallakpour, M. Dinari, J. Reinf. Plast. Compos. 32 (2013) 217–224, http://dx.doi.org/10.1177/0731684412467236.
[27] S. Deb, D. Sarkar, Indian J. Phys. 82 (6) (2008) 715–718.
[28] J.I. Hussain, S. Kumar, Z. Khan, Adv. Mater. Lett. 2 (2011) 188–194, http://dx.doi.org/10.5185/amlett.2011.1206.
[29] J. Lin, H. Lan, W. Zheng, Y. Qu, F. Lai, Nano 07 (2012) 1250048, http://dx.doi.org/10.1142/S1793292012500488.
[30] P.V. Kamat, J. Phys. Chem. B 106 (2002) 7729–7744.
[31] Y. Zhou, C.Y. Wang, Y.R. Zhu, Z.Y. Chen, Chem. Mater. 11 (1999) 2310–2312, http://dx.doi.org/10.1021/cm990315h.
[32] M. Raffi, J.I. Akhter, M.M. Hasan, Chem. Phys. 99 (2006) 405–409.
[33] S. Clemenson, L. David, E. Espuche, J. Polym. Sci Part A Polym. Chem. 45 (2007) 2657–2672, http://dx.doi.org/10.1002/pola.22020.
[34] F. Hajakbari, M. Ensandoust, Acta Phys. Pol. A 129 (4) (2016) 680–682, http://dx.doi.org/10.12693/APhysPolA.129.680.
[35] Y.S. Jung, Z. Sun, H.K. Kim, Appl. Phys. Lett. 87 (2005) 263116, http://dx.doi.org/10.1063/1.1850601.
[36] M. Voue, N. Dahmouchene, J. De Coninck, Thin Solid Films 519 (9) (2011) 2963–2967, http://dx.doi.org/10.1016/j.tsf.2010.12.109.
[37] X.C. Ren, S.M. Wang, F. Leung, P.K.L. Chan, Appl. Phys. Lett. 99 (043303) (2011) 1, http://dx.doi.org/10.1063/1.3617477.
[38] M.R. Johan, M. S.n M. Suan, N.L. Hawari, H.A. Ching, Int. J. Electrochem. Sci. 6 (2011) 6094–6104.
[39] A. Swami, P.R. Selvakannan, R. Pasricha, M. Sastri, J. Phys. Chem. B 108 (19269) (2004), http://dx.doi.org/10.1021/jp0465581.
[40] B. Karthikeyan, Physica B 364 (2005) 328–332, http://dx.doi.org/10.1016/j.physb.2005.04.031.
[41] S. Deb, D. Sarkar, Nanosci. Nanotechnol. Indian J. 5 (1) (2011) 13–16.
[42] A.S. Kutsenko, V.M. Granchak, Theor. Exp. Chem. 45 (5) (2009) 313–318.
[43] M. Abdelaziz, E.M. Abdelrazek, Physica B 390 (2007) 1–9, http://dx.doi.org/10.1016/j.physb.2006.07.067.
[44] P.K. Khanna, N. Singh, S. Charan, V.V.S. Subbarao, R. Gokhale, U.P. Mulik, J. Mater. Chem. Phys. 93 (2005) 117–121, http://dx.doi.org/10.1016/j.matchemphys.2005.02.029.
[45] A. Gautam, G.P. Singh, S. Ram, Synth. Met. 157 (2007) 5–10.
[46] R. He, X. Qian, J. Yin, Z.K. Zhu, J. Mater. Chem. 12 (2002) 3783–3786, http://dx.doi.org/10.1039/B205214H.
[47] R.A.R. Tricker, Introduction to Meteorological Optics, American Elsevier Publishing, New York, 1970, pp. 225–229.
[48] V. Amendola, O.M. Bakr, F. Stellacci, Plasmonics 5 (2010) 85–97, http://dx.doi.org/10.1007/s11468-009-9120-4.
[49] X. Yang, Wei He, S. Wang, G. Zhou, Y. Tang, J. Exp. Nanosci. 9 (6) (2014) 541–550, http://dx.doi.org/10.1080/17458080.2012.677548.
[50] A. Mooradian, Phys. Rev. Lett. 22 (1969) 5477.
[51] I. Saini, J. Rozra, N. Chandak, S. Aggarwal, P.K. Sharma, A. Sharma, Mater. Chem. Phys. 139 (2013) 802–810.